

Supplementary Information

S-1 Phase analysis of the samples

The phase of BN sample was identified by XRD pattern and FTIR spectrum. In Fig. S1, the diffraction peaks can be indexed to the (002) and (100) planes of hBN, no other impurity peaks can be observed. Here the (002) peak of hBN slightly shifted to lower angle, which reveals that high density structural defects may exist in the BN sample. In the FTIR spectrum (Fig. S2), the weak and broad peak at $\sim 3444\text{ cm}^{-1}$ comes from the absorption of adsorbed water, while the other two strong peaks at 1389 cm^{-1} and 808 cm^{-1} should be attributed to $\nu(\text{B-N})$ and $\delta(\text{B-N})$ modes of hBN. All these results indicate that the BN sample consists of single phase hBN.

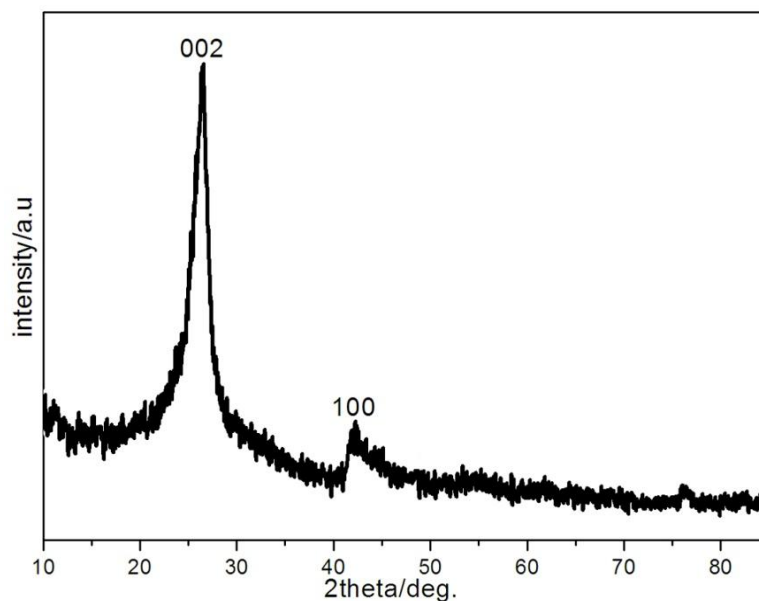


Fig. S1 XRD pattern of as-prepared BN sample.

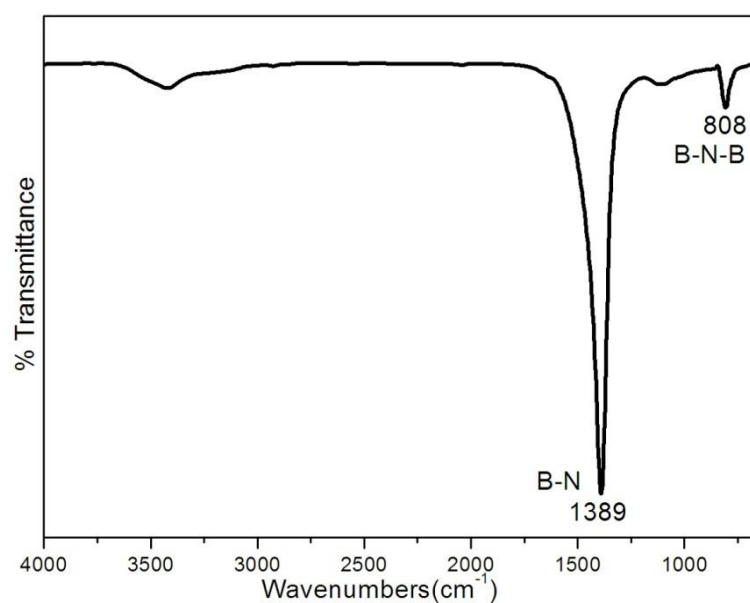


Fig. S2 FTIR spectrum of as-prepared BN sample.

S-2 HRTEM images of BNHSs

The shell structure of BNHSs was characterized by HRTEM. As shown in Fig. S3, the dominant shells consist of only a few graphene-like BN layers (4~9 layers).

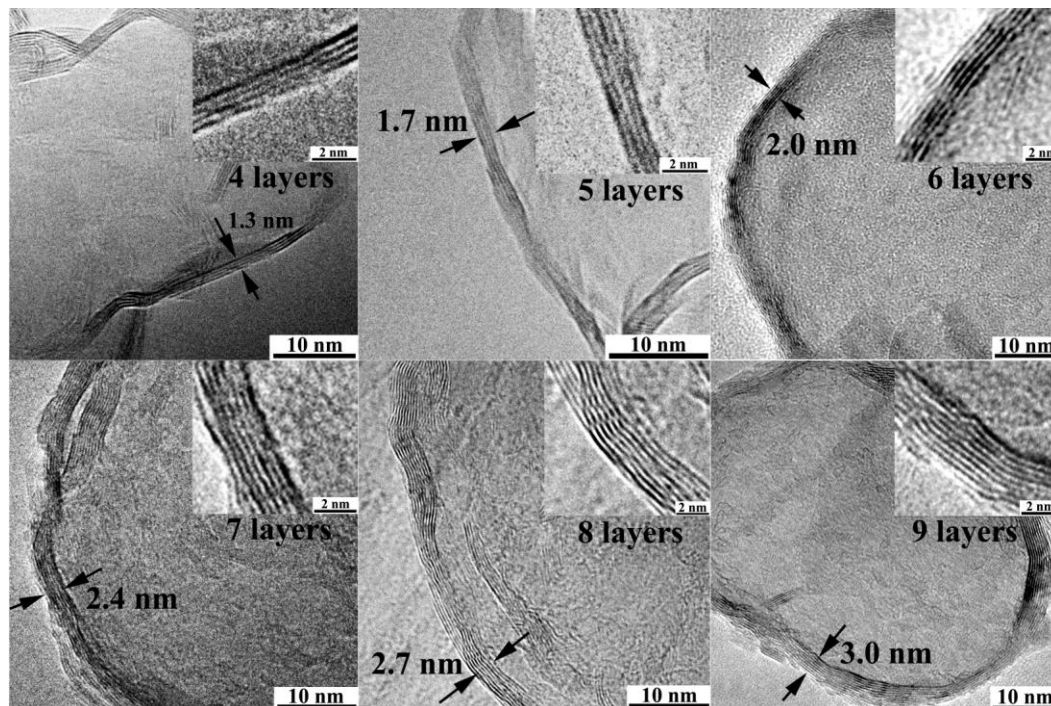


Fig. S3 HRTEM images of BNHSs with ultrathin shell (4~9 layers).

S-3 Comparison of hydrogen adsorption capacity per unit specific surface area (SSA) of different BN nanomaterials

A comparison of the adsorption capacities per unit SSA against SSA of BN nanomaterials is displayed in Fig. S4. It is quite clear that BNHSs C has the highest hydrogen adsorption capacity per unit SSA (1.90×10^{-2} wt.% $m^{-2} \cdot g$), which is much greater than those of the other BN nanomaterials.

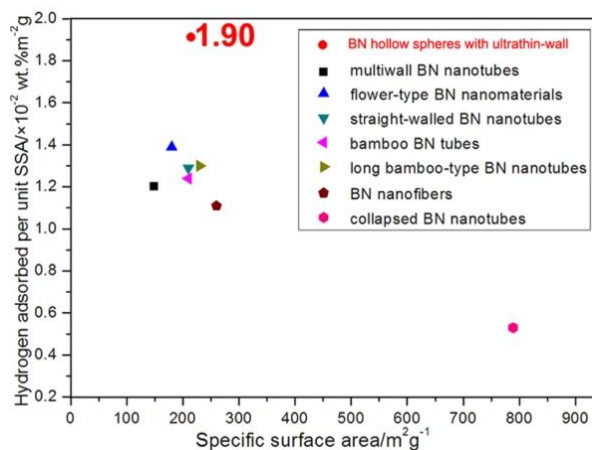


Fig. S4 Comparison of hydrogen adsorption capacities per unit SSA of different BN nanomaterials ^[1-5].

S-4 A schematic diagram of aromatic compounds adsorbing on the surface of BNHSs via non-covalent interaction

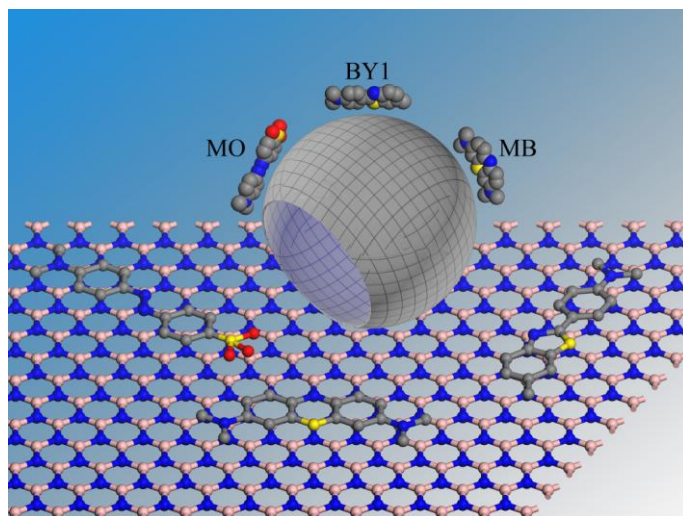


Fig. S5 A schematic diagram of aromatic compounds adsorbing on the surface of BNHSs via non-covalent interaction.

S-5 Adsorption performance of BNHSs C to methylene blue (MB)

Besides basic yellow 1 (BY1), BNHSs C also exhibited good performance in adsorbing methylene blue (MB) from wastewater. The concentration of MB in the solution quickly decreased when BNHSs C was added into the solution. The experimental data fit the Langmuir adsorption isotherm well, with correlation coefficient of 0.994. The maximum adsorption capacity is 116.5 mg/g. Furthermore, the BN (MB) composite can be easily recovered at 300 °C for 2 h in air (inset in Fig. S5).

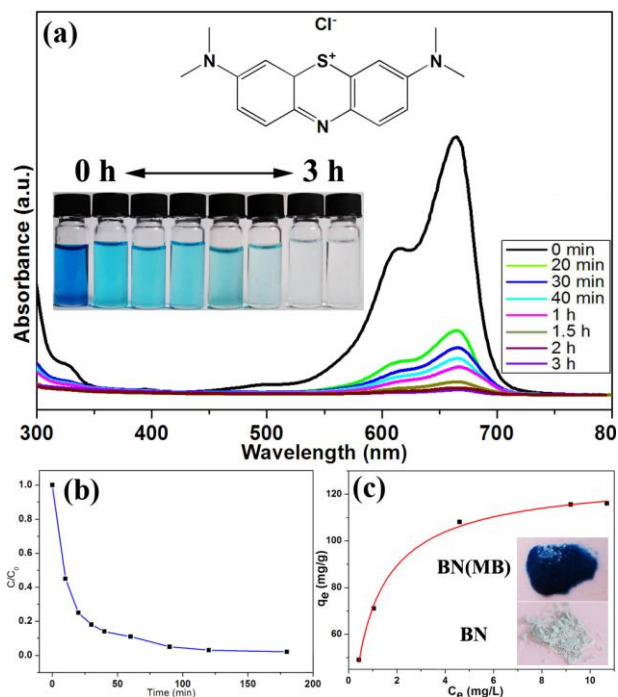


Fig. S6 (a) Absorption spectra and the photo (inset) of methylene blue (MB) aqueous solution (25 mgL^{-1} , 25 mL) after being mixed with BNHSs C (10 mg) for different intervals. The molecular structure of MB is presented in (a); (b) The adsorption rate of MB on BNHSs C; (c) The adsorption isotherm of MB on BNHSs C. Inset in (c) present the photos of BNHSs-MB composite before (upper) and after (bottom) recovering process.

S-6 BNHSs C selectively adsorb methyl orange (MO) from the mixed solution of MO and copper acetate

Similar to the situation of selectively adsorbing BY1 from the mixed solution of BY1 and CuSO_4 , BNHSs can also preferentially adsorb methyl orange (MO) from the mixed aqueous solution of MO and copper acetate (Fig. S7). After adding 4 mg BNHSs C into 10 mL mixed solution, all MO molecules are adsorbed while only small portion of Cu(II) ions has been adsorbed and removed from the solution.

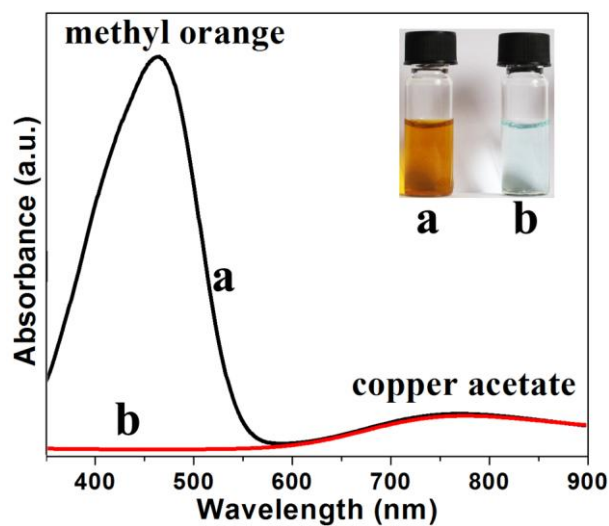


Fig. S7 Absorption spectra of mixed solution of methyl orange and copper acetate with presence of different amounts of BNHSs C. The volume of mixed solution is 10 mL, and the concentrations of methyl orange and $\text{Cu}(\text{CH}_3\text{COO})_2$ are 20 and 100 $\text{mg}\cdot\text{L}^{-1}$, respectively. (a) 0 mg BNHSs C; (b) 4 mg BNHSs C. Inset is the photos corresponding to the absorption spectra.

References

- [1] A.L.M. Reddy, A.E. Tanur, G.C. Walker, *Int. J. Hydrogen Energy*, **2010**, *35*, 4138;
- [2] R.Z. Ra, Y. Bando, H.W. Zhu, T. Sato, C.L. Xu, D.H. Wu, *J. Am. Chem. Soc.* **2002**, *124*, 7672;
- [3] C.C. Tang, Y. Bando, X.X. Ding, S.R. Qi, D. Golberg, *J. Am. Chem. Soc.* **2002**, *124*, 14550.
- [4] R.Z. Ma, Y. Bando, T. Sato, D. Golberg, H.W. Zhu, C.L. Xu, D.H. Wu, *Appl. Phys. Lett.*, **2002**, *81*, 5225-5227;
- [5] T. Terao, Y. Bando, M. Mitome, K. Kurashima, C.Y. Zhi, C.C. Tang, D. Golberg, *Phys. E*, **2008**, *40*, 2551-2555.